MPPT-Based Optimal NNC-*h*MOGA/BPA for Photovoltaic Water Pumping System

Rati Wongsathan
Department of Electrical Engineering, Faculty of Engineering and Technology, North-Chiang Mai University, 169 Nong Kaew, Hang Dong, Chiang Mai, Thailand 50230
Email: rati@northcm.ac.th

Ronnachai Phatchaiyo and Isaravuth Seedadan
Department of Fundamental Engineering and Electrical Engineering, Faculty of Engineering and Technology North-Chiang Mai University, 169 Nong Kaew, Hang Dong, Chiang Mai, Thailand 50230
Email: {ronnachai, isaravuth}@northcm.ac.th

***Abstract*—This paper proposes a Neural Network Controller (NNC) design based on the Maximum Power Point Tracking (MPPT) power-converter technique, and applied to a Photovoltaic Water Pumping System (PVWPS). To maximize the energy utilization and motor-pump efficiency, the proposed MMPT-NNC is optimized and trained through the hybrid of multi-objective genetic algorithm and back-propagation algorithm or *h*MOGA/BPA. By means of the genetic optimization, the number of NN parameters and the computational complexity can be significantly reduced by 31% and 18%, respectively. After determining the solutions of NN and relevant parameters, the performances of MPPT controllers are evaluated in terms of the tradeoff between transient response, stabilized MPPT accuracy, and energy utilization efficiency, under weather variations. As results, the proposed NNC-*h*MOGA/BPA provides a faster response without overshoot, a higher MPPT accuracy with negligible oscillations, and 10-40% more energy utilization efficiency as compared to the non-optimal NNC, and Perturb and Observe (P&O) method. Consequently, the motor-pump efficiency is maximized, including water discharge.**

***Index Terms*—neural network controller, multi-objective genetic algorithm, Maximum Power Point Tracking (MPPT), Photovoltaic Water Pumping System (PVWPS)**

I. Introduction

Due to global energy crisis, fuel shortage and air pollution, a Photovoltaic (PV) energy has become a promising renewable energy source in contributing to power production because of a large power density, and a few hours a day available in most outdoor locations. In rural or off-grid connected area, the PV system plays an important role in electricfication. PV Water Pumping System (PVWPS) among other PV applications is utilized to reduce the dependence on diesel fuel costs [1], [2]. To obtain an optimal PVWPS, the PV generator is necessary to operate at the Maximum Power Points (MPPs) that can also highly supply to the motor as load. Unfortunately, the locus of the MPPs strongly varies nonlinearly with the climatic chages, then achieving the MPP is not always guaranteed, especially under different adverse climatic conditions. To improve the efficiency of PVWPS, an MPP Tracking (MPPT)-based controller is incorporated.

Various MPPT controllers have been applied to the PV systems [3]-[13]. Generally, they are divided into two groups, i.e., conventional controllers, such as Perturb and Observe (P&O) method [3], and incremental conductance (IC) method [4]; and intelligent controllers, such as Neural Network Controller (NNC) [5], [6], Fuzzy Logic Controller (FLC) [5], Neuro-Fuzzy Controller (NFC) [7]. In practice, the conventional MPPT controllers are widely used due to their low cost and ease of implementation. However, they show an inefficient operation in failing to track the MPPs and by performing oscillations at the steady state leading to wasted energy. Alternatively, the MPPT-NNC performs the fast transient response against the rapid weather changes, and is able to track the MPP accurately with negligible oscillations when compared to the conventional MPPT controller [8]. However, the complexity is the one major drawback of MPPT-NNC. In addition, a number of training data, slow convergence, and local trap of system parameters from the Back-Propagation Algorithm (BPA) are the disadvantages. On the other hand, the MPPT-FLC and -NFC are outstanding to stabilize MPPT accuracy. However, a number of fuzzy rules do not contribute enough for accuracy improvement while increasing complexity. Furthermore, due to the conventional FLC design, i.e., generating fuzzy rules by the expert leading to the redundant rules, and adjusting parameters through trial and error, the optimal performance may not found [9].

Considering the NNCs applied to PVWPS [10]-[13], they are commonly trained using the BPA by choosing the learning rate (η) and momentum (α) from the expert. The different input types are used, such as the solar irradiance (G) [10], the output power (P_{PV}) from solar generator and motor speed (ω) [11], G and temperature (T) [12], and the global maximum power (P_{GMP}) and votage at GMP point (V_{GMP}) generated by the scaning algorithm (SCA) under partial shaded condition [13]. However, all

Manuscript received May 27, 2019; revised October 22, 2019.

doi: 10.18178/ijoee.7.2.51-57

the MPPT-NNCs mentioned above when using BPA are the disadvantages [14]. To overcome these problems, the system parameters were chosen from the expert without training in order to make the hidden layer output linearized [15], but this limits their full potential. Moreover, due to a number of hidden layers and hidden nodes in the NNC design resulting in computational complexity and the massive system parameters, a tuning through the conventional BPA may be ineffective. Recently, to avoid *the explosion of complexity*, the novel NNC applied to the tracking control problem is proposed [16]. In addition, the NNC containing only one adaptive parameter is introduced for the reduction of online computation [17]. Besides, the stochastic optimizations, such as Genetic Algorithm (GA), Particle Swarm Optimization (PSO), and others, play a role in simplifying the NNC design, e.g., NNC-GA [18], [19], NNC-PSO [20]. For the MPPT-NNC-GA, the number of hidden nodes is determined by GA [18], whereas in [19] GA is used to optimize the input dataset.

Motivated by the aforementioned effectiveness of the NNC-GA, the purpose of this work is to design the optimal MPPT-NNC using the hybrid Multi-Objective GA (MOGA) and BPA optimization, denoted by NNC-*h*MOGA/BP, for the PVWPS. To simplify the NN structure, the number of hidden nodes of single hidden layer is obtained through the experiment. Furthermore, to avoid the use of solar irradiance sensor which is more expensive and high-maintenance, the PV current (I_{PV}), PV voltage (V_{PV}) and ω are used as the inputs of NNC. In this fashion, the number of NN parameters (i.e. weights and biases) and their values, including the parameters of BPA (η and α), and other relevant parameters (i.e., the parameters of genetic operator, and objective function), are adjusted simultaneously, and derived through the *h*MOGA/BP, in order to achieve the optimal NNC. The proposed controller and the other existing MPPT-controllers, i.e., non-optimal NNC and P&O method, are carried out under fine weather with varying of G and T. Several criteria including transient response, MPPT accuracy, energy utilization, and computational complexity with regard to the multiplication counts are assessed to evaluate their performance.

In the following, the PVWPS is described in Section II. The design and optimization of NNC are presented in Section III. Section IV provides the results and discussion. Finally, Section V concludes this paper.

II. The PVWPS Description

A schematic model of typical PVWPS-controller used water storage tank instead of using battery storage (Fig. 1) is composed of PV generator, source of water, tank water, dc buck converter, Permanent Magnet dc Motor (PMDCM) coupled centrifugal pump and MPPT-controller. The pump flow rate (Q) and Total Dynamic Head (TDH) in a pump are predefined to estimate the capacity of pump, including rated power of motor, sizing PV, and capacitance (C) and inductance (L) in converter design. The MPPT-controller operates to produce the required Pulse Width Modulation (PWM) signal and corresponding duty ratio (D) for switching of buck converter in order to regulate the generated PV power from PV array to the motor under weather conditions of G and T. In this work, the circuit diagram of PVWPS-NCC is depicted in Fig. 2. In order to facilitate the most suitable approach for overall efficiency of the PVWPS, providing a more accurate and efficient model prior to installation is necessary.

To simulate the current-voltage (I-V) characteristics of the utilized PV generator, the PV array composed of N_s and N_p connected in series and parallel, respectively, is modeled using single diode equivalent circuit model [21] describing by 5 parameters, i.e., the photo-current (I_{ph}), diode saturation current (I_{sd}), series resistance (R_s), parallel or shunt resistance (R_{sh}), and the ideality factor of diode (n). The PV parameters are derived through the extracting method based on artificial intelligence technique as referred to [22].

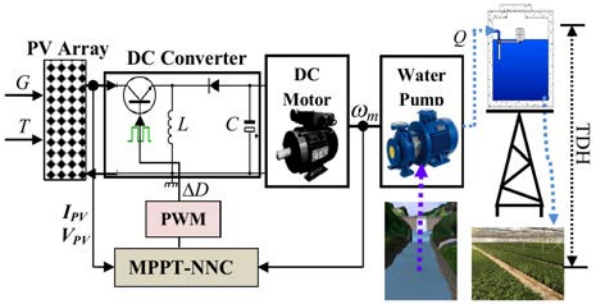

Figure 1. A typical PVWPS with MPPT-NNC.

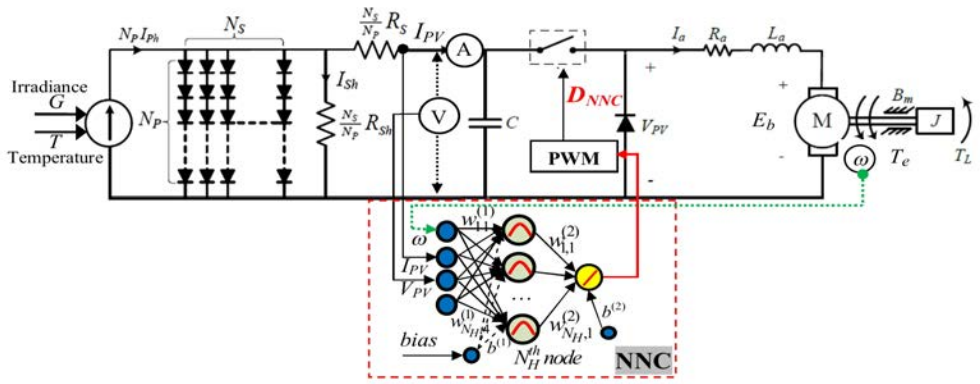

Figure 2. Schematic circuit diagram of PVWPS with the proposed MPPT-NN.

Using those obtained PV parameters, the output current of the PV array (I_{PV}) can be determined from the implicit expression [21] of

$$I_{PV}(G,T,V_{PV}) = N_P I_{ph} - N_P \times I_{sd}\left[\exp\left(\frac{qV_{temp}}{nK_BT}\right)-1\right] - \left(\frac{V_{temp}}{R_{sh}/N_P}\right) \quad (1)$$

where

$$I_{ph}(G,T) = \left[I_{sc} + K_I(T-T_0)\right]\left(\frac{G}{G_0}\right)$$

$$I_{sd}(T) = I_{sd,0}\left(\frac{T}{T_0}\right)^3 \times \exp\left[\frac{qE_g}{nk_B}\left(\frac{1}{T_0}-\frac{1}{T}\right)\right]$$

$V_{temp} = V_{PV}/N_S + I_{PV}R_S/N_P$, q is the electron charge, K_B is Boltzmann's constant, I_{sc} is the short circuit current at standard test conditions (STC; T_0=298 and G_0=1000), K_I is the temperature coefficient of I_{sc}, $I_{sd,0}$ is the saturation current at T_0, and E_g is the band gap energy of the semiconductor (eV).

The dc power generated from the PV array is supplied to the PMDCM under the driving torque of the centrifugal pump given by [23], $T_L=K_L\omega^k$, where K_L and k is the constant. At the steady state, i.e., dI_a/dt =0, and $d\omega/dt$=0, the power delivered from the PV $P_{PV}(G, T)$ to the motor can be derived as

$$P_{PV}(G,T) = \left(\frac{K_L^2R_a}{K_t^2}\right)\omega^{2k} + \left(\frac{2BK_LR_a}{K_t^2}+K_L\right)\omega^{k+1} + \left(\frac{B^2R_a}{K_t^2}+B\right)\omega^2 \quad (2)$$

where K_L and k is the constant of the load torque, I_a is the armature current, R_a is the armature winding resistance, L_a is the armature self-inductance, K_t is the torque constant, and B is the viscous torque constant losses**.**

The buck converter is employed to step down the PV voltage to a rated motor by changing the input resistance equal to motor load through the PWM signal generated from the MPPT controller. The design of MPPT-NNC using *h*MOGA/BPA is mentioned next section.

III. The Design of MPPT-NNC

The design procedure of the MPPT-NNC with the *h*MOGA/BPA optimization is shown in Fig. 3. The original structure of the MPPT-NNC (Fig. 4) abbreviated to NNC (3, N_H, 1) comprises 3 input nodes including V_{PV}, I_{PV} andω; N_H-hidden node, and the output node of the estimated-duty ratio (D_{NNC}) which is expressed as

$$D_{NNC} = f\left(\mathbf{W}^{(2)} \times g\left(\mathbf{W}^{(1)} \times \mathbf{X} + \mathbf{b}^{(1)}\right) + b^{(2)}\right) \quad (3)$$

where $\mathbf{X}=[V_{PV}, I_{PV}, \omega]^T$, $\mathbf{W}^{(1)}$ and $\mathbf{b}^{(1)}$ are (N_H×3)-weight matrix and N_H-bias column vector between input and hidden layer, respectively, $\mathbf{W}^{(2)}$ and $b^{(2)}$ are N_H-weight column vector and the bias between hidden and output layer, respectively, $g(\cdot)$ is hyperbolic tangent function and $f(\cdot)$ is linear function. Therefore, the number of NN parameters (weights and biases) is $5N_H$+1.

In order to determine the computational complexity of the NNC (3, N_H, 1) with regard to the multiplication counts, $g(\cdot)$ represented by Taylor series (TS) at $x=u$, i.e., $g(x)\sim(x-u)+(x-u)^3/3$, where $|x-u|\le\pi/2$, provides 3 multiplications, then the nonlinear transformation of hidden layer of NNC requires $3N_H$-multiplication, respectively. Therefore, the NNC provides total ($7N_H$)-multiplication including $3N_H$- and N_H-multiplication generated from input-hidden and hidden-output layer, respectively. To optimized the NNC, after normalizing the input variables, the N_{pop}-chromosome is randomly generated which each possesses vector entries with certain length of genes (parameters) of N_{bit}-length binary coding normalized within the specified range [-1, 1]. In the proposed encoding scheme all NN parameters (*w*'s and *b*'s) and relevant parameters, i.e., η, α, and the fitness constant (C_1), and parameter giving the percentage of contribution in the total fitness (C_2) in (4), are tabulated in Table I. The number of NN parameters are reduced through the set {0, 1} which is '0' means not consideration the accordingly parameter while '1' means to take the parameter into consideration.

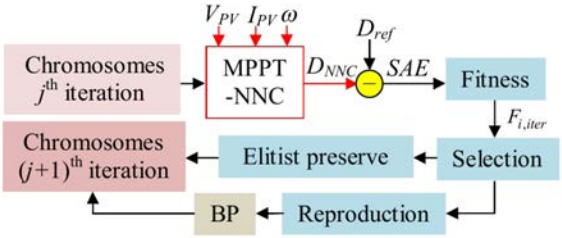

Figure 3. The procedure of NNC optimization using *h*MOGA/BP.

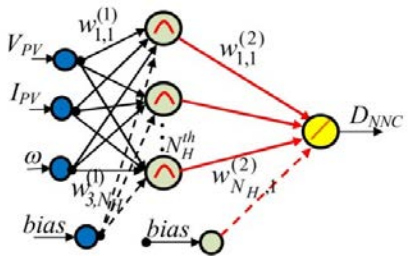

Figure 4. The structure of the optimized MPPT-NNC(3, N_H, 1).

TABLE I. Chromosome Representation for the NNC Optimization through MOGA

NNC/MOGA	Weights	Biases	Selected parameters	Relevant parameters
Variable	w	b	-	-
Gene	$w_{1,1}^{(1)},...,w_{3,N_H}^{(1)}, w_{1,1}^{(2)},...,w_{N_H,1}^{(2)}$	$b_1^{(1)},...,b_{N_H}^{(1)}, b_1^{(2)}$	{0,1}	η,α, C_1, C_2
Gene No.	$\|1\|\ldots\|3N_H\|3N_H+1\|\ldots\|4N_H\|$	$\|4N_H+1\|\ldots\|5N_H+2\|$	$\|5N_H+3\|\ldots\|10N_H+4\|$	$\|10N_H+5\|\ldots\|10N_H+8\|$

In the design, the number of hidden nodes is first determined through the experiment. The i^{th} chromosome is taken to compute the duty ratio at time k+1 ($D_{NNC,\,k+1}$). In the learning stage of the network, the weights and biases are updated using the *h*MOGA/BPA in order to minimize the Sum of Absolute Error (SAE) of the differences between the estimated and desired duty ratios. The MOGA seeks to maximize the multi-criteria fitness function, $F_{i,j}$, (4) composed of the weighted of SAE and the reduction of the number of NN parameters in terms of ratio of the initial number of parameters (NP_0) to the current number of parameters (NP_{iter}),

$$F_{i,j} = \frac{C_{1,i,j}}{\sum_{k=1}^{N_{SP}} \lambda^{N_{SP}-k} \mid D_{target} - D_{NNC}^{k,i} \mid} + C_{2,i,j} \frac{NP_0}{NP_{i,iter}} \qquad (4)$$

where $\lambda \in (0, 1]$ is a forgetting factor and N_{SP} is the maximum samples per an iteration. The parent chromosomes based on their high fitness values are selected to generate the offspring by two methods. First, the elitism method is used to retain the best chromosome about 10%. Second, the roulette wheel method is used by assigning a higher probability of selection to individuals with higher fitness values that passes through the reproduction process, i.e., crossover and mutation with probability of P_C and P_M, respectively. The BPA is applied to the individual offspring as the supervised training using the inputs-output sequences obtained from the simulations in Section 2. The resultant individuals refined by BPA and an elite are rearranged according to the fitness values. Thus, the chromosomes in the $(j+1)^{th}$ iteration are obtained. The genetic process is repeated until meeting the maximum iteration (N).

IV. Simulation Results

In this work, the water source is a well. The Total Dynamic Head (*TDH*) is assumed to be 10 m. The average water requirement is 80 m^3/day for estimated available 6 hrs a day, therefore the flow rate (Q) for the pump is 15 m^3/h and is varied in the range 10-50 m^3/h. The total water storage capacity is 240 m^3 for a minimum of three days water use. According to the specifications of the electrical devices utilized in the PVPWS (Table II) and the required flow rate, the output power of the PV array is varied in the range 300-1,300 W, then PV modules are connected in series in order to increase the voltage driving the DCPM motor. Therefore, N_S is sufficiently selected as 9. The I_{PV}-V_{PV} characteristic curves of the PV array obtained from the experiment (Fig. 5(a)) under varying of G and constant T (20°C) against the motor load are shown in Fig. 5(b). It is seen that the operating points (red circle) deviate away from the MPPs (black dot) under adverse conditions (low G and high T).

For the buck converter design, L and C are estimated to be 60 µH and 14 µF, respectively, by method referred to [24], when the maximum current is allowed to up to 10 A. The peak to peak inductor ripple current and capacitor ripple voltage is assumed to be 5%, the PWM switching frequency is set as 200 kHz. The maximum input and output voltage are 200 V and 120 V, respectively.

TABLE II. Electrical Specifications of PV Module, PMDCM and Centrifugal Pump

Description	Specification
PV module	
- Type	Polycrystalline silicon
- Model	SHARP ND-130T1J
- Rated power (P_{max})	130 W
- Maximum power voltage (V_{mp})	17.4 V
- Maximum power current (I_{mp})	7.48 A
- Open circuit voltage (V_{OC})	22.0 V
- Short-circuit current (I_{SC})	8.09 A
PV circuit parameters [22]	
- I_{ph}	8.01 A
- I_s	8.77 µA
- R_s	16 mΩ
- R_{sh}	690.72 Ω
- n	1.877
PMDC motor [11]	
- Rated motor voltage (V_a)	120 V
- Rated motor current (I_a)	9.2 A
- Rated motor speed (ω)	2.61 rpm
- Armature resistance (R_a)	1.5 Ω
- Armature inductance (L_a)	0.2 H
- Voltage constant (K_t)	0.676V/rad/sec
- Torque constant (K_L)	0.676 Nm/A
- Motor friction (A_m)	0.2 Nm
Centrifugal pump [11]	
- Moment of inertia (J)	0.0236 Kg m^2
- Viscous friction coefficient (B)	0.00238 Nm/(rad/sec)
- Load torque constant (K_e)	0.00039 Nm/(rad/sec)
- Load friction (A_L)	0.3 Nm

To optimize the NNC under the given conditions of G and T, I_{PV} and V_{PV} were varied from 1 to 8 A, and from 5 to 175 V in increments of 1 and 10, respectively, and the corresponding D_{NNC} was measured for each case. The train:test data was set as 70:30 and N=200. To avoid the local optimum traps of solutions, λ was set as 0.99. The parameters of GA were set as follows: N=200, N_{SP}=144, N_{pop}=10, N_{bit}=12, P_C=0.85 and P_M=0.15.

(a)

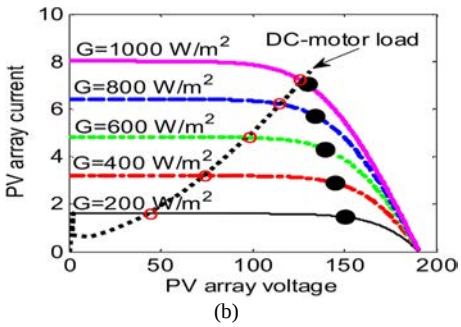

(b)

Figure 5. (a) Experimental setting of G and T using pseudo-solar for the utilized PV-module, (b) The I_{PV}-V_{PV} characteristics of PV array (9-module connected in series) and motor load characteristics.

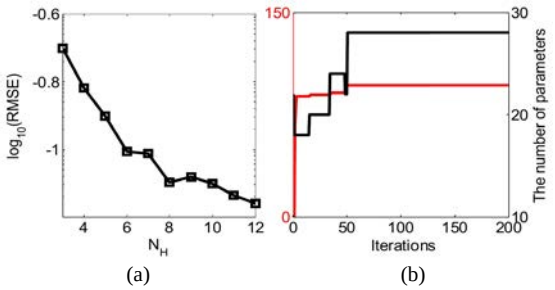

Figure 6. (a) RMSE against N_H and (b) The convergence profile of the fitness and reduction of the number of parameters through MOGA.

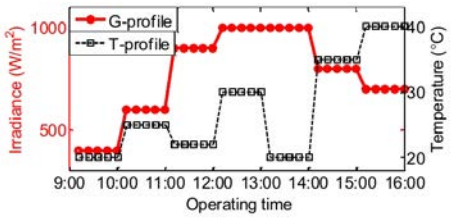

Figure 7. The weather variations of irradiance and temperature.

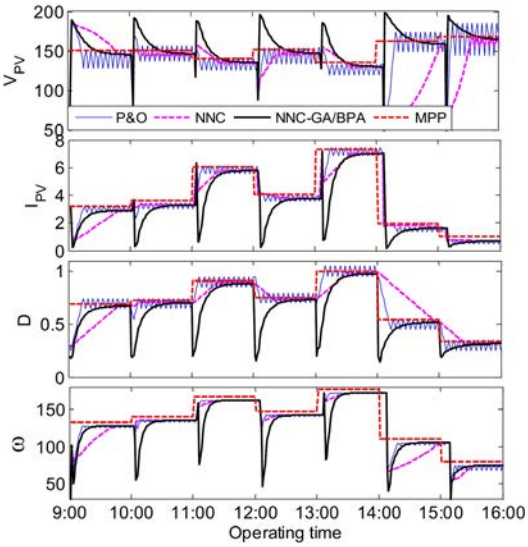

Figure 8. The regulated I_{PV}, V_{PV}, D and ω under varying of G and T.

The NNs are started with the small network and gradually added hidden nodes as long as their performances are not improved. From the consideration from the plotting of RMSE against the number of hidden nodes in Fig. 6(a), N_H is selected as 8, then MPPT-NNC(3, 8, 1) yields 41 parameters which are tuned through the *h*MOGA/BPA in order to maximize (4). The number of multiplications of the MPPT-NNC is 56. However, due to the maximizing problem of Eq. (4) with over parameter reduction, the solutions may not satisfy the optimal solution, then the parameter $C_{1,i}$ and $C_{2,i}$ are required to weight the terms in Eq. (4). Therefore, the high performance can be found for determining these appropriate values.

From the experiment, C_1 and C_2 vary in the range of 1-15 and 10-150, respectively. As can be seen in Fig. 6(b), the fitness values increase with iteration and saturate at the 50^{th} iteration, the number of parameters of NNC is reduced from 41 to 28 (17-$w^{(1)}$, 5-$b^{(1)}$, 5-$w^{(2)}$, 1-$b^{(2)}$). Therefore, the proposed optimal NNC provides 46-multiplication resulting in computational complexity reduction by 18% when compared with the non-optimal NNC. The MATLAB\SIMULINK software is used for simulation of the PVWPS-controller. The system was simulated to verify the functionality and performance of the proposed MPPT-NNC (3, 8, 1) and to quantify how the proposed controller increased the system efficiency compared with other controllers under different weather conditions. Through the test, the performances of the controllers are investigated under fine weather (Fig. 7) where G and T are varied between 200-1000 W/m^2, and 20-40°C, respectively. The measures are recorded every 12 minutes. From the control results depicted in Fig. 8, the cases show the good matching between I_{PV}, V_{PV}, ω and D with the optimal values under weather variations. Then, the motor speed reaches to the optimal values corresponding to the MPPs of the PV array leading to water discharge maximization. However, the control results of the P&O are not appreciated due to its high fluctuations.

To investigate the transient and steady-state response of the controllers (Fig. 9), the P&O provides fast response time, but more oscillations causing more power waste, whereas the optimal NNC provides the faster transient response as compare to the non-optimal NNC, and reaches the MPPs with negligible oscillations. Furthermore, the NNCs perform better than the P&O with regard to the stabilized MPPT accuracy.

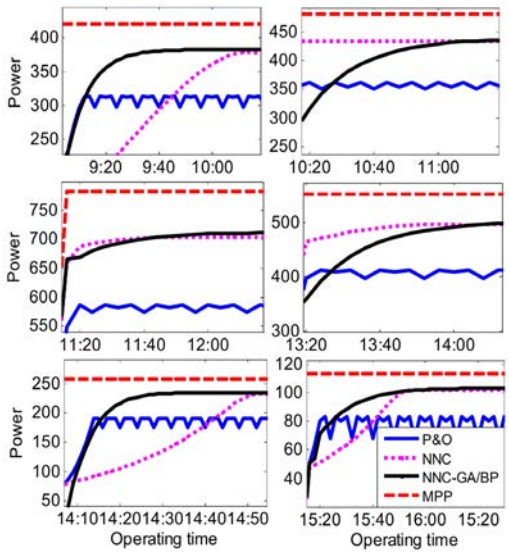

Figure 9. Transient and steady state response of the controllers.

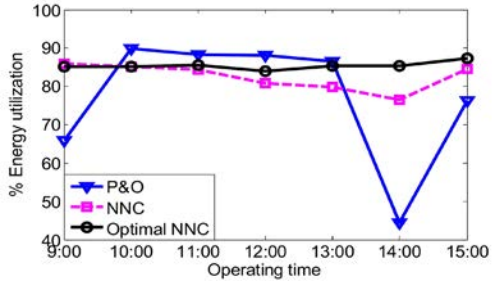

Figure 10. Comparison of energy utilization between MPPT-controllers.

In order to compare the energy utilization between the controllers, the energy utilization efficiency ($\eta_{utilize}$) over interval $[t_i, t_f]$ is defined as

$$\eta_{utilize} = \int_{t_i}^{t_f} \left(P_{MPPT}(t) / P_{MPP}(t) \right) dt \quad (5)$$

where P_{MPPT} represents the extracting power obtained from the controller. From Fig. 10, the proposed optimal-NNC, non-optimal NNC, and P&O method averagely provide about 86%, 81% and 77% energy utilization efficiency, respectively.

V. Conclusions

In this work, the optimal NNC called NNC-*h*MOGA/BPA is derived through the *h*MOGA/BPA. By MOGA optimization, the number of NN parameters, and the comuputational compelxity are significantly reduced. The parameters are further fine-tuned for achieving the optimal NNC through the BPA. When implemented in PVWPS under weather variations, the proposed NNC outperforms the rest. Tradeoff by several criteria including energy utilization efficiency are assessed to support above statement. Continuing the work, the MPPT technique based on FLC and NFC with optimization is investigated for comparing the performances with that of the proposed NCC.

Acknowledgment

This research was supported by the Research Institute of North-Chiang Mai University, Chiang Mai Thailand.

References

[1] K. Sudararaju and M. Hariprabh, "Implementation of intelligent grid-interfaced PV with dc-dc boost converter topology for agricultural water pumping system," *Int. J. of Pure and Applied Mathematics*, vol. 118, no. 20, pp. 2147-59, 2018.

[2] M. J. M. Rao, M. K. Sahu, and P. K. Subudhi, "PV based water pumping system for agricultural sector," *Material Today: Proceeding*, vol. 5, pp. 1008-1016, 2018.

[3] A. Harrag, A. Titraoui, H. Bahri, and S. S. Messalti, "Photovoltaic pumping system-Comparative study analysis between direct and indirect coupling mode," *Technologies and Materials for Renewable Energy, Environment and Sustainability AIP Conf. Proc*., vol. 1814, 2017.

[4] B. Kumar, Y. K. Chauhan, and V. Shrivastava, "Performance analysis of a water pumping system supplied by a photovoltaic generator with different maximum power point tracking techniques," *Songklanakarin J. of Science and Technol.*, vol. 36, no. 1, pp. 107-113, 2014.

[5] A. Mathew and A. I. Selvakumar, "MPPT based stand-alone water pumping system," in *Proc. Int. Conf. on Comp., Commun. & Elect. Technol.-ICCCET2011*, 2011, pp. 455-460.

[6] H. Abu-Rub, A. Iqbal, S. K. M. Ahmed, F. Z. Peng, Y. Li, and G. Baoming, "Quasi-Z-Source inverter-based photovoltaic generation system with maximum power tracking control using ANFIS," *IEEE Trans. on Sustainable Energy*, vol. 4, no. 1, pp. 11-20, 2013.

[7] N. Priyadarshi, *et al*., "Maximum power point tracking for brushless DC motor driven photovoltaic pumping system using hybrid ANFIS-FLOWER pollination optimization algorithm," *Energies*, vol. 11, no. 5, pp. 1-16, 2018.

[8] R. Wongsathan and A. Nuangnit, "Optimal hybrid neuro-fuzzy based controller using MOGA for photo-voltaic (PV) battery charging system," *Int. J. of Control, Automation and Systems (IJCAS)*, vol. 16, no. X, pp. 1-11, 2018.

[9] R. Wongsathan, "Performance of hybrid fuzzy and neuro-fuzzy controller with MOGA based MPPT for a solar PV module on various weather conditions," *Engng. J. CMU*., vol. 24, no. 2, pp. 161-175, 2017.

[10] M. Veerachary and N. Yadaiah, "ANN based peak power tracking for PV supplied DC motors," *Solar Energy*, vol. 69, no. 4, pp. 343-350, 2000.

[11] F. Aashoor and F. Robinson, "Maximum power point tracking of PV water pumping system using artificial neural based control," in *Proc. 3rd Renewable Power Generation Conference*, 2014.

[12] M. Yaichi, M. K. Fellah, and A. Mammer, "A neural network based MPPT technique controller for photovoltaic pumping system," *Int. J. of Power Electronics and Drive System (IJPEDS)*, vol. 4, no. 2, pp. 241-255, 2014.

[13] L. Bouselham, M. Hajji, B. Hajji, and H. Bouali, "A MPPT-based ANN controller applied to PV pumping system," in *Proc. Int. Renewable and Sustainable Energy Conf. (IRSEC)*, Marrakech, Morocco, 2017.

[14] R. Rojas, *Neural Networks: A Systematic Introduction*, New York: Springer-Verlag, 1995.

[15] M. T. Makhloufi, Y. Abdessemed, and M. S. Khireddine, "An efficient ANN-based MPPT optimal controller of a DC/DC boost converter for photovoltaic systems," *J. of Control, Measurement, Electronics, Computing and Communications*, vol. 57, no. 1, pp. 109-119, 2017.

[16] C. Wu, J. Liu, Y. Xiong, and L. Wu, "Observer-based adaptive fault-tolerant tracking control of nonlinear nonstrict-feedback systems," *IEEE Trans. Neural Netw. Learn. Syst.*, vol. 29, no. 7, pp. 3022-3033, 2018.

[17] S. Yin, H. Yang, H. Gao, J. Qiu, and O. Kaynak, "An adaptive NN-based approach for fault-tolerant control of nonlinear time-varying delay systems with unmodeled dynamics," *IEEE Trans. Neural Netw. Learn. Syst.*, vol. 28, no. 8, pp. 1902-1913, 2017.

[18] A. A. Kulaksiz and R. A. Akkaya, "A genetic algorithm optimized ANN-based MPPT algorithm for a stand-alone PV system with induction motor drive," *Solar Energy*, vol. 86, no. 9, pp. 2366-2375, 2012.

[19] A. A. Kulaksiz and R. Akkaya, "Training data optimization for ANNs using genetic algorithms to enhance MPPT efficiency of a stand-alone PV system," *Turk J. Elec. Eng. & Comp. Sci*., vol. 20, no. 2, pp. 241-254, 2012.

[20] C. Y. Lee, Y. X. Shen, J. C. Cheng, Y. Y. Li, and C. W. Chang, "Neural networks and particle swarm optimization based MPPT for small wind power generator," *Int. J. of Elect. and Comput. Engineering*, vol. 60, pp. 17-23, 2009.

[21] M. A. D. Blass, J. L. Torre, E. Prieto, and A. Garcia, "Selecting a suitable model for characterizing photovoltaic devices," *Renewable Energy*, vol. 25, pp. 371-380, 2002.

[22] R. Wongsathan and I. Seedadan, "Artificial intelligence and ANFIS reduced rule for equivalent parameter estimation of PV module on various weather conditions utilize for MPPT," *Int. J. of Renewable Energy*, vol. 12, no. 1, pp. 38-55, 2017.

[23] A. Braunstein and A. Komfeld, "Analysis of solar powered electric water pumps," *Solar Energy*, vol. 27, no. 3, pp. 235-240, 1981.

[24] S. Oprea, M. C. Tanase, and A. florescu, "PV charger system using a synchronous buck converter," in *Proc. SNET*, Bucharest, Romania, 2012, vol. 3, no. 1, pp. 328-333.

Rati Wongsathan was born in Lamphum, Thailand, in 1976. He received his B. Eng. (Hons), M. Eng. in Electrical Engineering, and M. Sc. in Applied Mathematics from Chiang Mai University (Chiang Mai, Thailand) in 1996, 2001 and 2005, respectively. He is now pursuing his Ph. D. degree at King Mongkut's Institute of Technology Ladkrabang, KMITL (Bangkok, Thailand). He has been a lecturer in Faculty of Engineering and Technology at North-Chiang Mai University (NCU), Thailand, since 2000. His research interests include nonlinear and adaptive control, and channel equalization

Ronnachai Phatchaiyo was born in Phitsanulok, Thailand, in 1972. He received his B. Sc. (Physics) in 1997 from Naresuan University (Phitsanulok, Thailand) and M. Sc (Applied Geophysics) in 2005 from Chiang Mai University (Chiang Mai, Thailand). He has been a lecturer in Fundamental Engineering at North-Chiang Mai University (NCU) since 2005. His research interests include seismic refraction tomography and artificial intelligence.

Isaravuth Seedadan was born in Sakon Nakhon, Thailand, in 1969. He received the B. Eng. (Hons) in Electronics Engineering from Vongchavalitkul University (Nakhon Rachasima, Thailand), M. Eng. degree in Electrical Engineering from King Mongkut's Institute of Technology Ladkrabang, KMITL (Bangkok, Thailand). He joined the Department of Electrical Engineering, North-Chiang Mai University (NCU), Chiang Mai, Thailand, as a Lecturer since 2003. His research interests include the renewable energy and electronics design.